crystals

MDPI

Article

Effects of Recycled Fine Aggregates and Inorganic Crystalline Materials on the Strength and Pore Structures of Cement-Based Composites

Sung-Ching Chen [1,*], Si-Yu Zou [2] and Hui-Mi Hsu [3]

[1] School of Civil and Architectural Engineering, East China University of Technology, Nanchang 330013, China
[2] Taiwan Construction Research Institute, Taipei 23146, Taiwan; siyuzou@tcri.org.tw
[3] Department of Materials Science and Engineering, National Dong Hwa University, Hualien 97401, Taiwan; hmhsu@gms.ndhu.edu.tw
* Correspondence: jaosn314@ecut.edu.cn; Tel.: +86-15995807147

Abstract: Concrete is porous; the partial pores in the internal structure of concrete are generated by hydration products, such as calcium hydroxide, dissolved in water. External harmful substances in the form of gases or aqueous solutions can penetrate concrete. The destruction of the internal structure of concrete leads to problems such as shortening of the service life of concrete as well as the corrosion and poor durability of steel. To improve the pore structure of concrete, a material can be added to concrete mixtures to cause the secondary hydration of the hydration products of cement. This reaction is expected to reduce the pore volume and increase the density of concrete. For existing concrete structures, inorganic crystalline materials can be used to protect the surface and reduce the intrusion of external harmful substances. In this study, the water–binder ratio was 0.4 and 0.6. Three inorganic crystalline materials and recycled fine aggregates (0%, 10%, 20%, and 30% replacement of natural aggregates by weight) were used in the same cement-based composites. The results indicated that all specimens had a high total charge-passed value, and inorganic crystalline material C provided superior protection for green cement-based composites.

Keywords: recycled fine aggregates; sealer; durability; mercury intrusion porosimetry

Citation: Chen, S.-C.; Zou, S.-Y.; Hsu, H.-M. Effects of Recycled Fine Aggregates and Inorganic Crystalline Materials on the Strength and Pore Structures of Cement-Based Composites. *Crystals* **2021**, *11*, 587. https://doi.org/10.3390/cryst11060587

Academic Editors: Yi Bao, Salman Siddique, Wei-Ting Lin and Trilok Gupta

Received: 30 April 2021
Accepted: 21 May 2021
Published: 23 May 2021

1. Introduction

Concrete is currently the most widely used construction material; however, its service life varies in different environments. Long-term corrosive environments containing materials such as carbon dioxide, chloride, and sulfate can damage or deteriorate concrete [1–7] and shorten its service life. Steel corrosion is a common failure phenomenon observed in concrete structures. The expansion of corrosion products produces internal tension, which causes the protective layer to crack and accelerates the penetration of harmful substances into the concrete, leading to the insufficient durability of reinforced concrete structures. Taiwan's older reinforced concrete structures are due for demolition or reinforcement. Maintenance and reinforcement technology for concrete structures is a crucial topic in construction engineering. The unsuitable repair of concrete structures affects the social and economic development of an area as well as human safety. The main hazards of concrete cracks are affecting the bearing capacity and safety of the structure, affecting the waterproof of the structure, and affecting the durability and service life of the structure.

Traditional concrete has many negative environmental effects. The concept of green concrete has been developed to reduce the impact of concrete on the environment. Green concrete can be produced using recyclable and renewable resources to reduce environmental pollution. Moreover, green concrete can coexist with the natural environment to achieve sustainable development. The term "green" encompasses energy conservation and environmental sustainability [8–11]. The addition of recycled materials to concrete to

improve its workability, strength, durability, and volume stability [12] can create economic benefits in the field of civil engineering.

Considerable construction waste is produced every year in major public and private construction projects. Concrete accounts for the largest proportion of construction waste. To achieve sustainable development, advanced countries are actively engaged in the recycling of construction waste. Taiwan has limited land and a dense population; therefore, the recycling of construction waste in Taiwan can promote not only its reduction but also sustainable resource utilization. It can also alleviate the problems of construction waste stacking, limited burial space for construction waste, and insufficient construction resources [13].

A total of 70% of the natural aggregate supply in Taiwan is used in civil engineering. In addition to increased environmental awareness, difficulties in procuring earth and rock have led to shortages in raw construction materials. The amount of construction waste produced per year in Taiwan is estimated to be more than 10 million tons. A large amount of recycled concrete waste can be used as recycled aggregates to slow damage to the environment and achieve sustainable resource utilization.

Recycled aggregates are waste concrete blocks produced during processes such as building demolition, pavement repair, concrete production, and engineering construction. After concrete is crushed, screened, graded, and mixed in certain proportions, the formed aggregates are called recycled coarse or fine aggregates. Since recycled materials are applied in recycled aggregates, these aggregates have similar characteristics to those of green concrete. Waste concrete has various sources. Currently, the main sources of waste concrete are concrete blocks produced from aging or expired building demolition, the relocation of municipal engineering structures, or new construction or reconstruction of major infrastructure; unqualified products from commercial concrete plants, prefabricated component plants, or concrete that was returned for some reason; scattered concrete produced during the construction and decoration of new building structures; complete concrete test blocks or components tested by laboratories and the scientific research institutions of construction units; and waste concrete produced by building collapse due to natural disasters or human factors [14].

The recycled aggregates obtained from crushed waste concrete contain natural aggregates and old cement pastes. The recycled aggregates have a specific gravity of approximately 2.2–2.5, a theoretical density of approximately 1200–1400 kg/m^3, and a water absorption rate of less than 10%. Compared with natural concrete materials, recycled concrete materials have lower specific gravity, higher porosity, and higher water absorption. The reason for this phenomenon is that recycled concrete materials are usually made from crushed waste concrete blocks formed during building and bridge demolition. Therefore, the surfaces of recycled concrete materials are flat, angular, rough, and porous. Studies have indicated that by adopting an appropriate mix design, the engineering properties and workability of recycled concrete can be made similar to those of natural concrete [15]. Several researchers have reported that the use of RFA as a replacement of natural river sand exhibits no negative effect on the durability of the normal strength concrete, i.e., the resistance to chloride ion ingress [16] and carbonation [17], provided the RFA content remains below 30% of natural sand. It is generally accepted in the previous research that in spite of reduced mechanical performance and marginally affected durability, the use of RFA in producing recycled fine aggregates concrete is possible, provided the RFA replacement ratio is within the optimum range along with good curing conditions [18].

Inorganic crystalline concrete materials are mainly composed of cement, silica sand, and other compound additives. After being mixed with an appropriate amount of water, these materials are coated on the surfaces of concrete structures to protect their bodies. Such materials are mainly painted or sprayed, which is convenient for construction, and they are widely used for various concrete structures [19]. Micropores exist in the protective layer of cementitious systems. These pores allow water vapor to pass through the protective layer,

preventing freeze–thaw damage to the coating. Four types of cementitious system exist: the metal salt, chemical additive, polymer, and permeable crystalline cementitious systems.

According to the GB 18445-2001 standard [20], permeable crystalline cementitious waterproofing materials include cement, silica sand, and other special compound additives that are mainly used for waterproofing concrete structures. The active substances in the material components are transported with water through the concrete. These substances form crystals with the hydration products of cement and block capillary pores and microcracks, which results in the enhancement of the water permeability and consistency of concrete. Then, water and gas permeabilities of concrete are major indicators to evaluate the ability of this material to prevent the penetration of aggressive agents such as carbon dioxide (CO_2) or chlorides as well as the transfer of water vapor due to drying of the material [21].

Concrete surfaces act as protective layers [22] within a depth of 30 mm from the surface layer, and a coating material is used on the concrete surface. Drying or a chemical reaction, hardening, and the formation of a protective layer that covers the concrete surface can protect or repair the surface of a concrete structure and improve its appearance. The life cycle of concrete can be extended, and its maintenance and management costs can be reduced using economical and convenient coating materials. Table 1 presents the reasons for treating concrete surfaces with sealing. According to the coating mechanism and composition, concrete surface coatings are classified as sealers, pore-lining coatings, pore-blocking coatings, and rendering coatings (Table 2).

Table 1. Causes of concrete surface sealing treatment [23].

Purpose	Causes of Surface Coating Treatment	Application or Location
Preventing direct deterioration	Chemical action	Corrosive chemicals
	Physical action	Freeze–thaw damage and erosion wear
Preventing steel corrosion caused indirectly	Decrease in the pH value of concrete	Concrete neutralization
	Loss of protection by passive protection film	Coastal environment and chloride erosion
Limiting surface contact	Waterproof measures	Poor structural design
	Gas barriers	Water vapor or sulfur dioxide
	Easy to clean and decontaminate	Factory or hospital floors and walls
Maintaining appearance	Color	Building facades
	Reflection processing	Tunnels and car parks
	Prevention of mold growth	Walls and floors
	Anti-graffiti coating or treatment	Help with graffiti removal
	Uniformity after repair	Recovery processing
Improving security	Skid resistance	Floor and road use
	Prevention of static electricity	On manufacturing floors
	Road marking	Indication or road marking

Table 2. Coating material with common mechanisms [23].

Type	Species	Characteristics
Coatings or sealers	Acrylic Butadiene copolymer Epoxy resin Polyester resin Polyethylene copolymer Polyurethane	They can modify appearances They can be isolated from liquid and gas invasion They are often used to protect the outermost layer Their subsequent maintenance is difficult Their wear resistance is poor
Pore-lining treatment	Silicones Siloxane Silane Silicone resins	They are unfavorable in high-temperature environments It can prevent erosion through water or chloride ions It can be used in road structure protection. Corrosion and wear resistance are poor in this treatment It does not affect the appearance of the concrete surface
Pore-blocking treatment	Silicate Silicofluoride Crystal growth materials	It enables resistance to liquid, gas, chemical attack, and abrasion The protective effect depends on the porosity of concrete The pore has good adhesion and long-term effect. Such coatings are the first protective layer of the concrete substrate.
Rendering	Plain and polymer-modified cement-based mortars	The coating provides a barrier effect of certain thickness. It can reduce the passing rate of moisture It allows the development of resistance to sulfate attack It has a wide range of applications

Cement mortar, which is a typical porous composite material, has varying pore size and shape. Pores are scattered in cement mortar and are an important factor affecting the ion transfer rate. According to their sizes, pores are subdivided into compaction, entrapped air, capillary, and gel pores [24]. The surface of cement mortar has the ability to transfer ions. When the contact angle between cement mortar and the atmosphere is small, water from the air can easily invade the surface of cement mortar along the capillary pores. Moreover, external harmful substances can be transported through water into cement mortar, affecting its mechanical properties and durability. According to [25], the crucial processes in cement mortar transmission include water transmission under hydrostatic pressure, water transmission caused by the capillary phenomenon, particle diffusion caused by the concentration gradient, and particle transmission caused by water movement. The transportation properties of external substances in cement mortar are mainly dependent on its pore structure; thus, pore size, volume, and connectivity in cement mortar affect the aforementioned properties.

An effective method of maintaining the durability of concrete is controlling the pore transport characteristics of materials, which mainly depend on the pore structure and pore size in concrete. The pore structure of concrete has a considerable influence on its strength and permeability. The pores in water-based composite materials can be divided into three categories according to their size [23]: (1) pores larger than 50 nm, which are called macropores; (2) pores 2–50 nm large, which are called mesopores; and (3) pores smaller than 2 nm, which are called micropores. Macropores and mesopores are generally called capillary pores, and they have a considerable influence on the physical properties of materials. Small pores are generally called colloidal pores and have a considerable influence on the drying shrinkage and creep behavior of materials. Thus, pore size, distribution, volume, and continuity in concrete affect the transmission characteristics of external substances that enter the concrete [26]. To improve the pore structure of concrete, in addition to water as well as coarse and fine materials that meet different specifications and standards, Portland cement or other mineral admixtures are added to concrete to increase its compactness and reduce its permeability [27].

In this study, construction waste is used as aggregate, and waste concrete is recycled as recycled aggregate. The practice of green concrete has greatly improved the environmental protection. In order to improve the durability of green concrete, inorganic crystalline coating is used. Inorganic crystalline coating can effectively reduce the pores of concrete, and also greatly reduce the probability of concrete failure. Thus, concrete protection affects its durability. In addition to changing the composition of concrete materials (e.g., by using pozzolanic materials), external water vapor can be prevented from being absorbed by the capillary pores of concrete to change the pore size and block tortuous paths [28–34]. The paper discusses the protective effect of the coating with mortar. The effect of the coating on the pore protection can be understood through mortar. Three types of inorganic crystalline materials were used in this study to test the mechanical properties, permeability, and microproperties of mortars containing recycled aggregates. The results of this study can serve as a reference for future research regarding which material provides superior surface protection for concrete.

2. Materials and Methods

2.1. Materials

2.1.1. Cement

In this study, Portland I cement from Taiwan Cement Company (Hualien, Taiwan) was adopted. The characteristics of this cement meet the specifications of the National Standards of the Republic of China (CNS) 61.

2.1.2. Natural Fine Aggregates

Natural fine aggregates were obtained from the Lanyang River (Yilan, Taiwan). According to the American Society for Testing and Materials (ASTM) C33 [35], the fineness

modulus (FM) of these aggregates is 2.8. According to ASTM C128 [36], the specific gravity [saturated surface dry (SSD)] and water absorption of the aforementioned aggregates are 2.56% and 1.85%, respectively.

2.1.3. Recycled Fine Aggregates

The recycled fine aggregates used in this study were obtained from Zunhong Environmental Protection Co., Ltd. (Keelung, Taiwan). According to ASTM C33 [35], the FM of these aggregates is 2.43. According to ASTM C128 [36], the SSD specific gravity and water absorption of the aforementioned aggregates are 2.42% and 6.16%, respectively.

2.2. Mix Design and Test Methods

For the setting of the mortar number, the first code is the W/C of mortar specimens and the second code is the crystalline material used, which is set to T, K, and C, as presented in Table 3. The T crystalline material was obtained from Kryton International Inc. (Vancouver, BC, Canada); the K crystalline material was procured from KÖSTER BAUCHEMIE AG (Aurich, Germany); and the C crystalline material was obtained from Jiawurong Industrial Co., Ltd (Taipei, Taiwan). Under the action of water, the active chemicals contained in cement-based permeable crystalline waterproof materials are brought into the surface pores of the structure through the erosion of surface water to the internal structure, and they react with free calcium oxide in mortar to form water-insoluble calcium sulfoaluminate ($3CaO{\cdot}Al_2O_3{\cdot}CaSO_4{\cdot}32H_2O$) permeable crystals. The crystal absorbs water and expands in the pores of the structure, which makes the surface layer of the mortar structure gradually form a dense impermeability area, and it greatly improves the impermeability of the whole structure. The third code involves the replacement of 10%, 20%, or 30% of the natural aggregates with recycled fine aggregates and the control factor group. The first code is related to the control factor group. In accordance with the research goal and the examination of the relevant literature, water–cement ratios of 0.4 and 0.6 were used for the cement mortar in the pilot test.

Table 3. Description of the adopted inorganic crystalline materials.

Type	Characteristic
T crystalline material	Flexibility greater than 900% Can be used for waterproofing balconies and roofs Unaffected by stagnant water
K crystalline material	Crack self-repairing function Restrains chloride ions and protects steel bars Can be used in drinking water facilities and is gray and nontoxic
C crystalline material	Remarkable waterproofing effect of the deep basement and continuous wall Waterproof valve foundation can effectively block moisture and maintain dryness Simple construction, can be painted or sprayed, and nontoxic nature

Table 4 presents the experimental variables. Three types of inorganic crystalline materials (T, K, and C) were used to coat the surface of the test body. Then, recycled fine aggregates were used to replace 0%, 10%, 20%, and 30% of the natural aggregates. The N mark indicates an unsealed sample. The test age was set to 7, 28, and 56 days. Three specimens of each mixture were required for each test in this study. The designed proportions of materials in the cement mortar are presented in Table 5. The design mix ratio of cement mortar depends on the amount of fine aggregates and T, K, C, or N coating.

Table 4. Test variables.

Type	Variables
W/C	0.4 and 0.6
Crystalline material	T, K, C, and N
Amount of recycled aggregate replacing natural aggregate (%)	0%, 10%, 20%, 30%
Maintenance conditions	Curing with saturated lime water

Table 5. Designed proportions in cement mortar.

Mix No.	w/c	Cement	Fine Aggregates	Recycled Fine Aggregate	T	K	C
4T0	0.4	1	1	0	V		
4T1	0.4	1	0.9	0.1	V		
4T2	0.4	1	0.8	0.2	V		
4T3	0.4	1	0.7	0.3	V		
4K0	0.4	1	1	0		V	
4K1	0.4	1	0.9	0.1		V	
4K2	0.4	1	0.8	0.2		V	
4K3	0.4	1	0.7	0.3		V	
4C0	0.4	1	1	0			V
4C1	0.4	1	0.9	0.1			V
4C2	0.4	1	0.8	0.2			V
4C3	0.4	1	0.7	0.3			V
4N0	0.4	1	1	0			
4N1	0.4	1	0.9	0.1			
4N2	0.4	1	0.8	0.2			
4N3	0.4	1	0..7	0.3			
6T0	0.6	1	1	0	V		
6T1	0.6	1	0.9	0.1	V		
6T2	0.6	1	0.8	0.2	V		
6T3	0.6	1	0.7	0.3	V		
6K0	0.6	1	1	0		V	
6K1	0.6	1	0.9	0.1		V	
6K2	0.6	1	0.8	0.2		V	
6K3	0.6	1	0.7	0.3		V	
6C0	0.6	1	1	0			V
6C1	0.6	1	0.9	0.1			V
6C2	0.6	1	0.8	0.2			V
6C3	0.6	1	0.7	0.3			V
6N0	0.6	1	1	0			
6N1	0.6	1	0.9	0.1			
6N2	0.6	1	0.8	0.2			
6N3	0.6	1	0..7	0.3			

The main test items and reference standards were divided into three categories: mechanical properties, permeability, and characterization properties. The mechanical properties of ϕ 10 × 20 mortar were tested according to ASTM C39m-12 [37]. According to ASTM C642-13 [38], ϕ 10 × 5 mortar was prepared for an absorption test. The ϕ 10 × 5 mortar was prepared according to BS 1881 [39] for an initial surface water absorption test. This mortar was prepared according to ASTM C1202 [40] for a rapid chloride penetration test (RCPT). Moreover, according to ASTM d4404-10 [41], 1 × 1 × 1 mortar was prepared for a mercury intrusion porosimetry (MIP) test. The coating is protected by coating on the outer layer of mortar specimen, as shown in Figure 1.

3. Results and Discussion

3.1. Compressive Strength

The test results are displayed in Figures 2 and 3. When the water–binder ratio was low, C was used as a coating material and recycled fine material was used to replace 0%. The strength of 7 days, 28 days, and 56 days is 24.83%, 32.89%, and 41.99% higher than that of recycled fine material. The compressive strength was higher at a low water–binder ratio than at a high water–binder ratio for all the test groups. Moreover, the compactness was higher at a low water–binder ratio than at a high water–binder ratio. At the same water–binder ratio, material C had higher compressive strength than did the other materials

for all curing ages. The initial compressive strength of material C was marginally greater than those of the other materials. For the same water–binder ratio and coating material, the effects of different proportions of recycled aggregate substitution on the compressive strength were compared. The highest compressive strength was obtained when material C was used as the coating material and the amount of replacement was 0%. Thus, the surface protection can be increased using C with 0% recycled substitution at a low water–binder ratio.

Figure 1. Schematic diagram of specimen sealing method.

The 28-day compressive strength reached 32.12 MPa. The strength requirement was 30 MPa when the water–binder ratio was low, C was used as the coating material, and the amount of recycled aggregate substitution was 20%. When the water–binder ratio was high and the other conditions were unchanged, the compressive strength reached 30 MPa in 56 days. When the water–binder ratio was low, the 28-day strength of material C was 4.92% higher than that of material K and 18.96% higher than that of material T. When the water–binder ratio was high, the 56-day strength of C was 0.11% higher than that of K and 13.88% higher than that of T.

Concrete coatings are widely used to improve the durability of reinforced concrete structures in order to prevent and control reinforcement corrosion in chlorides containing environment. Cement-based coatings, as well as organic-based coatings, act as a physical barrier to the penetration of water, ions, and gases [42]. The coating can reduce the pores on the surface of mortar, improve the compactness, and indirectly improve the compressive strength of mortar.

When the water–binder ratio was low, the 28-day compressive strengths of materials C, K, and T were 21.33%, 17.26%, and 2.92% higher than those of the uncoated samples, respectively, when the recycled fine aggregates replaced 20% of the natural aggregates. When the water–binder ratio was high and the other conditions remained unchanged, the 28-day compressive strengths of the C, K, and T coatings were 28.83%, 28.18%, and 20.45% higher than those of the uncoated samples, respectively, when the recycled fine aggregates replaced 20% of the natural aggregates. The aforementioned results indicate that the compressive strength increased by a greater extent under a high water–binder ratio than under a low water–binder ratio.

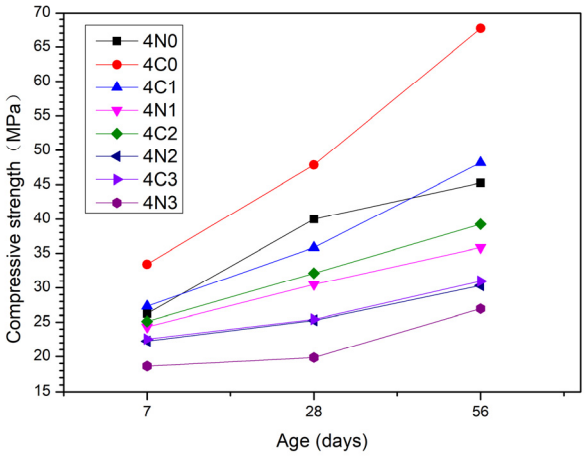

(**a**) C crystalline material

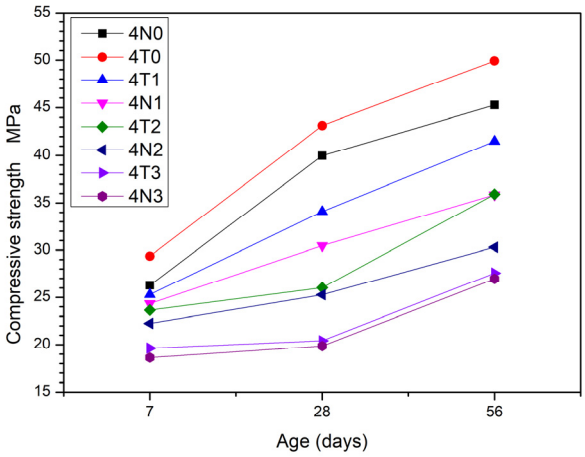

(**b**) T crystalline material

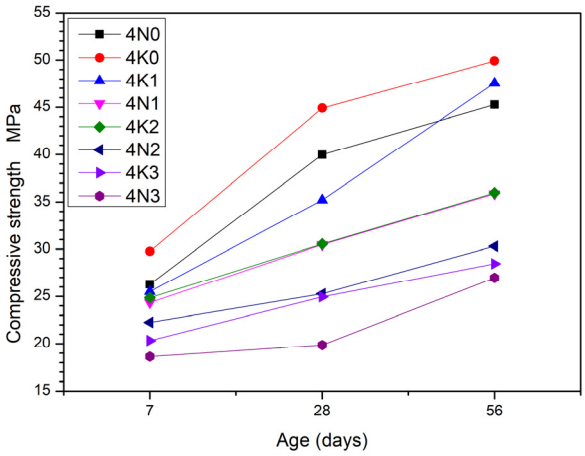

(**c**) K crystalline material

Figure 2. Compressive strength of cement mortar when W/C = 0.4.

3.2. Absorption Test

The porosity of the specimens was measured under oven-dry conditions and SSD. The saturated water absorption decreased with an increase in specimen age because the pores of the specimens were gradually filled in during the curing and hydration reaction and the compactness of the specimens increased. The results of the porosity test are illustrated in Figures 4 and 5. The saturated water absorption was lower under a low water–binder ratio than under a higher water–binder ratio. Thus, the compactness was higher at a low water–binder ratio than it was at a high water–binder ratio. Under the same water–binder ratio, the saturated water absorption of C was lower than that of the other materials. This result indicates that C is superior to the other adopted inorganic crystalline materials. At the same water–binder ratio and with C as the coating material, the saturated water absorption was the lowest for 0% recycled aggregate substitution, indicating that the compactness decreased with an increase in recycled aggregate substitution. The aforementioned results indicate that the best densification and surface protection effect can be obtained under a low water–binder ratio, 0% recycled aggregate substitution, and the use of C as a coating material.

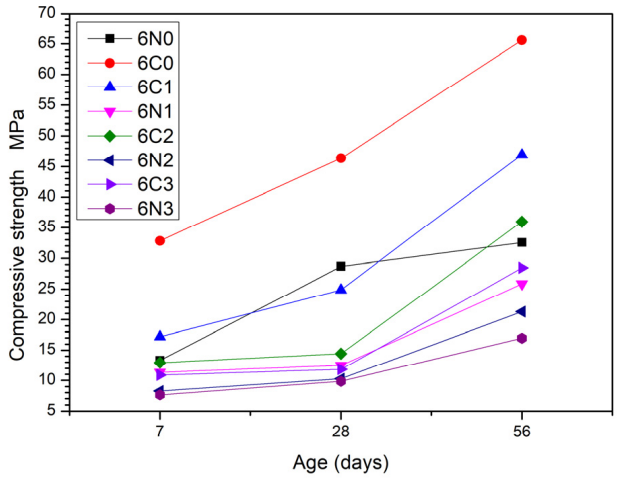

(**a**) C crystalline material

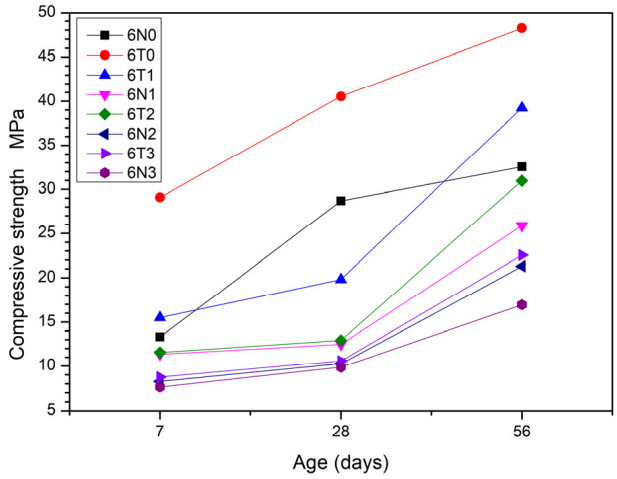

(**b**) T crystalline material

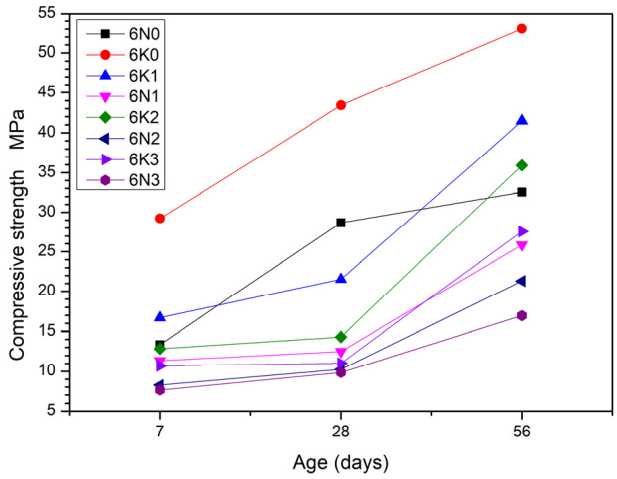

(**c**) K crystalline material

Figure 3. Compressive strength of cement mortar when W/C = 0.6.

When the water–binder ratio was low, the 28-day water absorption of the samples coated with K, T, and C was 20.05%, 16.20%, and 11.06% lower than that of the uncoated samples, respectively. When the water–binder ratio was high, the 28-day water absorption of the uncoated samples was 56.67%, 47.23%, and 39.94% higher than that of the samples coated with K, T, and C, respectively. The aforementioned results indicate that the water absorption was lower at a high water–binder ratio than at a low water–binder ratio. Moreover, the water absorption of the samples coated with T was lower than that of the control group.

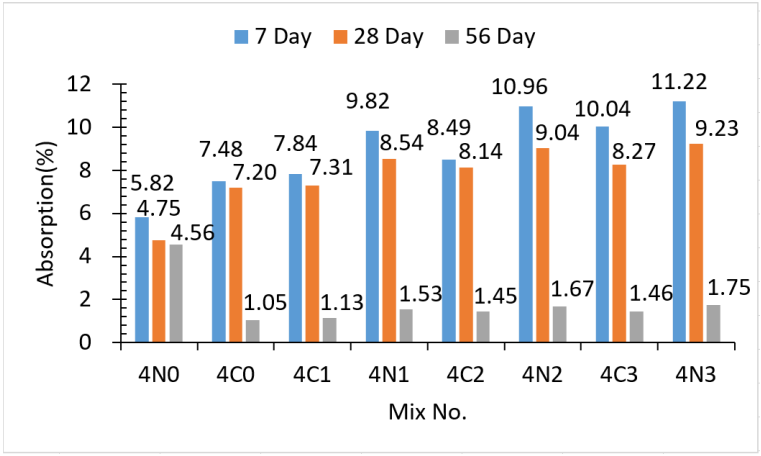

(**a**) C crystalline material

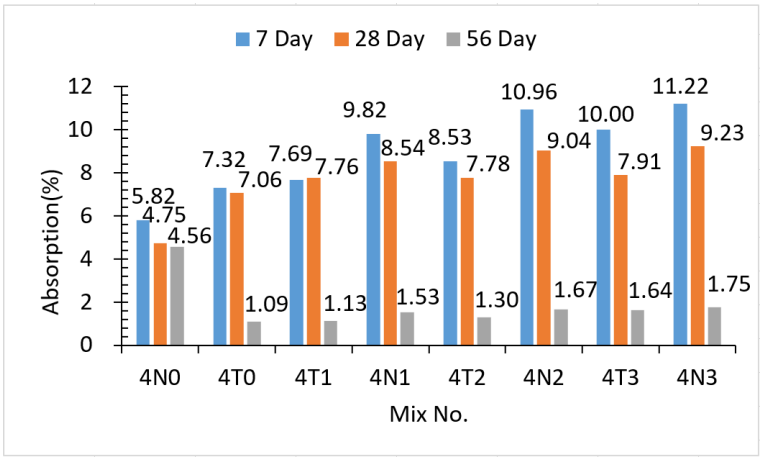

(**b**) T crystalline material

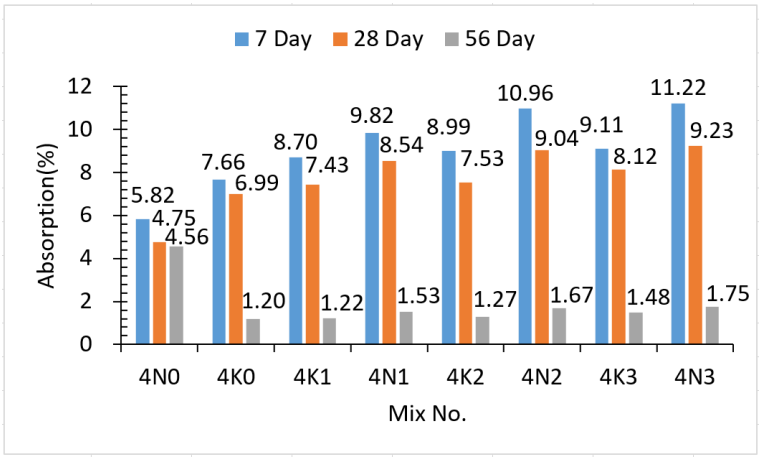

(**c**) K crystalline material

Figure 4. Saturated water absorption of cement mortar when W/C = 0.4.

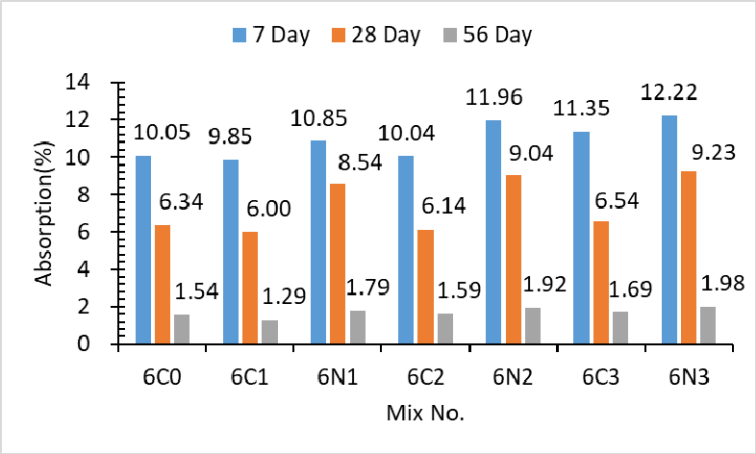

(**a**) C crystalline material

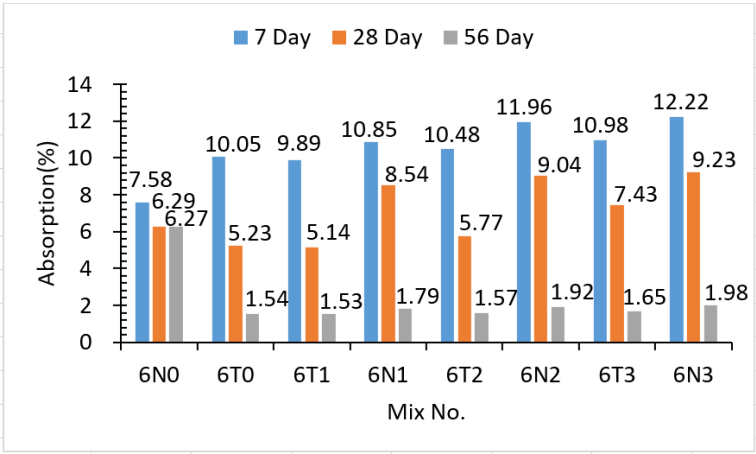

(**b**) T crystalline material

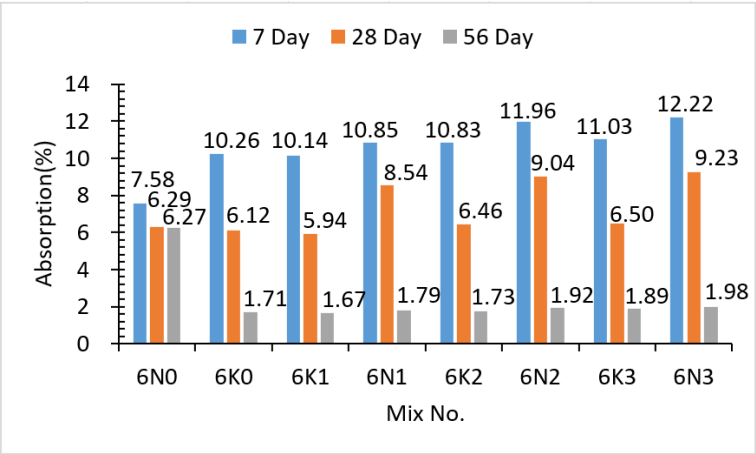

(**c**) K crystalline material

Figure 5. Saturated water absorption of cement mortar when W/C = 0.6.

3.3. Initial Surface Water Absorption Test

The surfaces of the specimens were mostly composed of capillary pores. The number of capillary pores and the compactness of the specimens could be inferred from the results of the surface water absorption test. The test results are displayed in Figures 6–11. The surface water absorption was lower at a low water–binder ratio than at a high water–binder

ratio, indicating that the number of capillary pores and the compactness were higher when the water–binder ratio was low. Under the same water–binder ratio, the surface water absorption of C was the lowest.

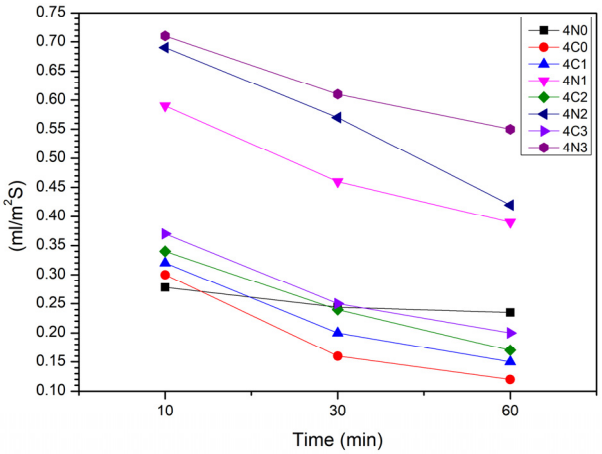

(**a**) C crystalline material

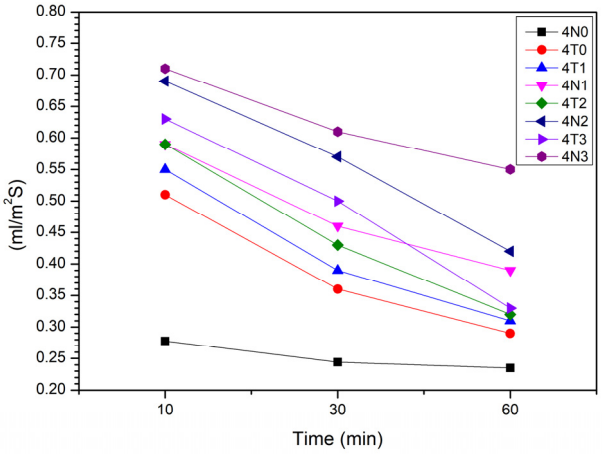

(**b**) T crystalline material

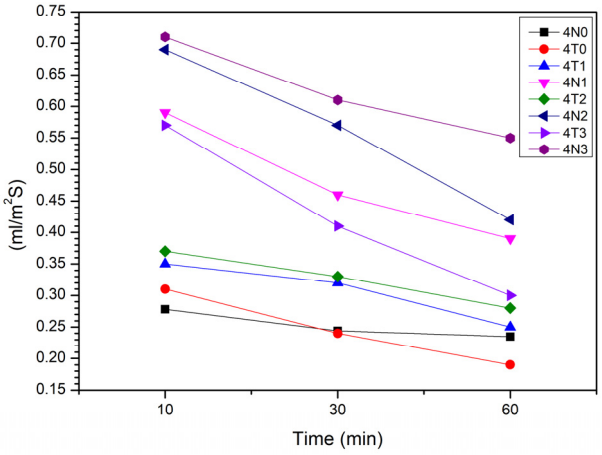

(**c**) K crystalline material

Figure 6. Initial surface water absorption of cement mortar after 7 days when W/C = 0.4.

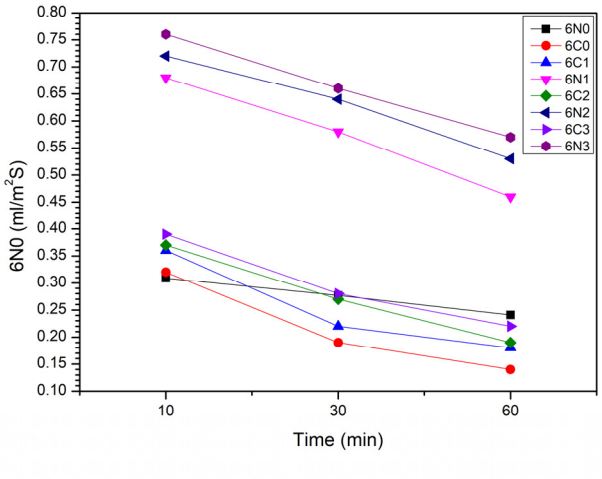

(**a**) C crystalline material

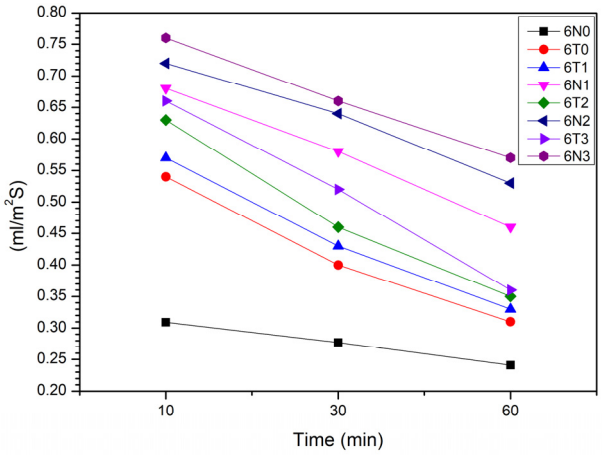

(**b**) T crystalline material

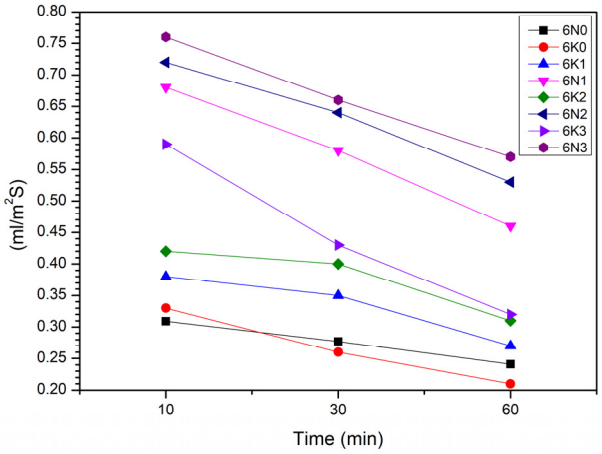

(**c**) K crystalline material

Figure 7. Initial surface water absorption of cement mortar after 7 days when W/C = 0.6.

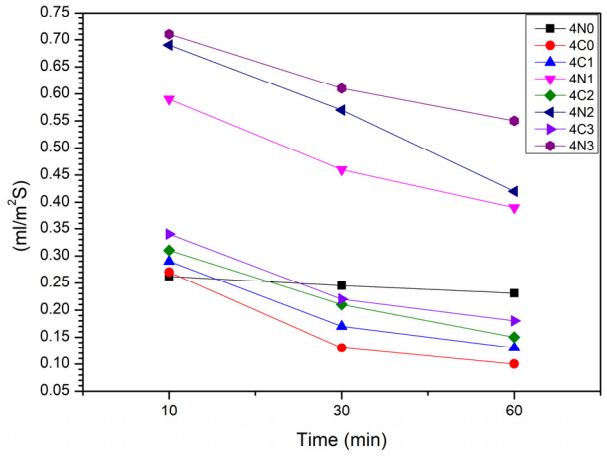

(**a**) C crystalline material

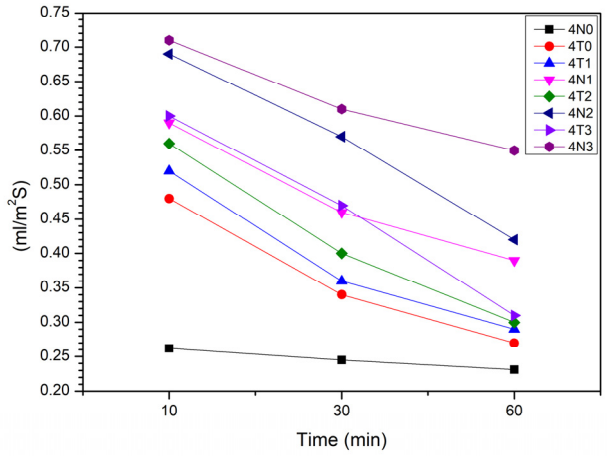

(**b**) T crystalline material

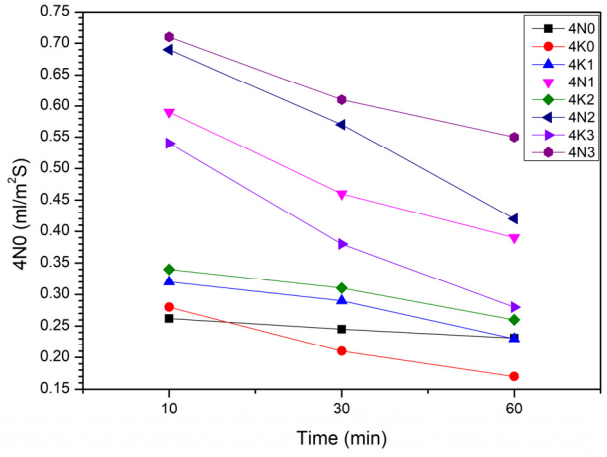

(**c**) K crystalline material

Figure 8. Initial surface water absorption of cement mortar after 28 days when W/C = 0.4.

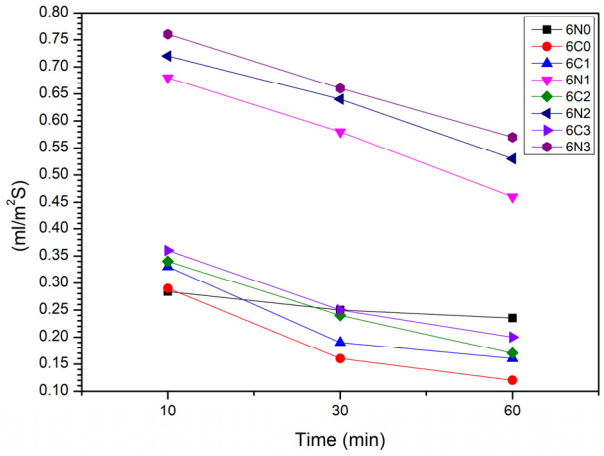

(**a**) C crystalline material

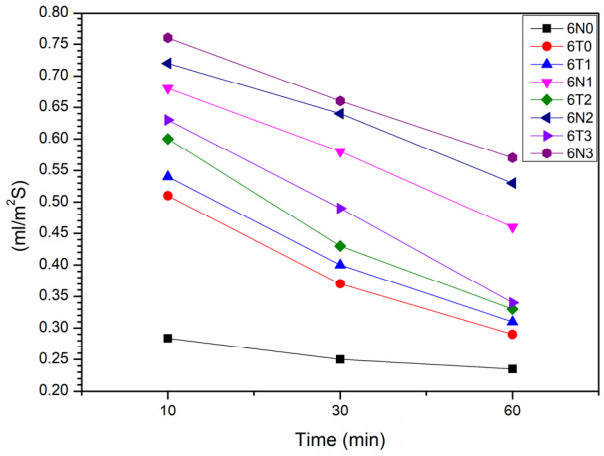

(**b**) T crystalline material

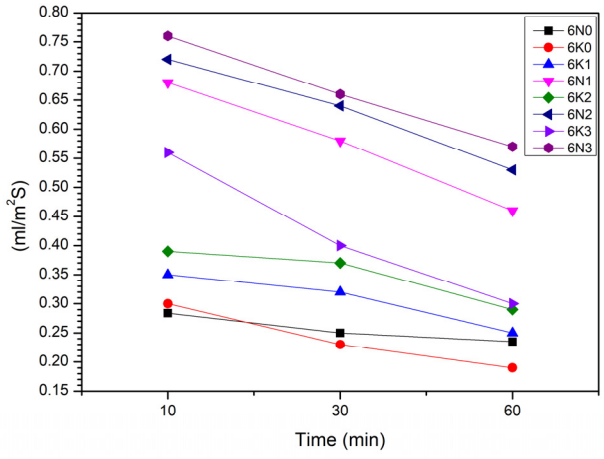

(**c**) K crystalline material

Figure 9. Initial surface water absorption of cement mortar after 28 days when W/C = 0.6.

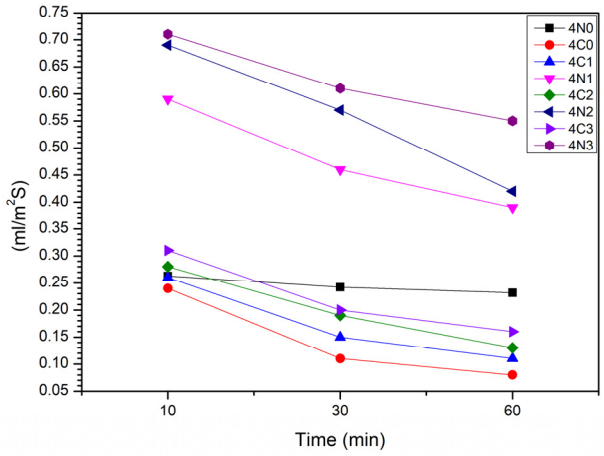

(**a**) C crystalline material

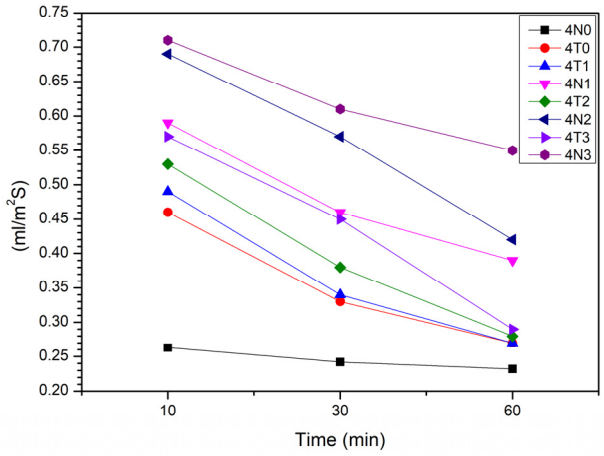

(**b**) T crystalline material

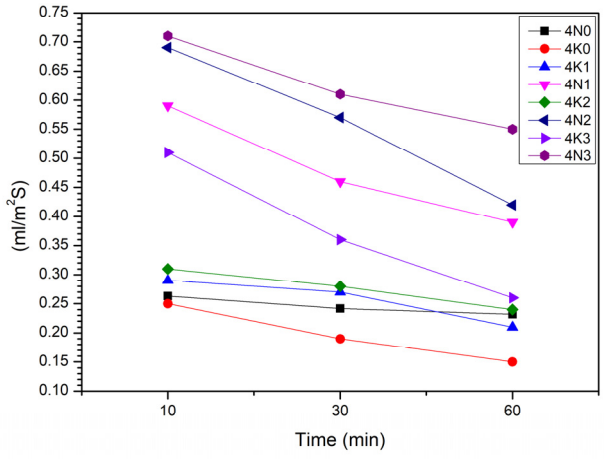

(**c**) K crystalline material

Figure 10. Initial surface water absorption of cement mortar after 56 days when W/C = 0.4.

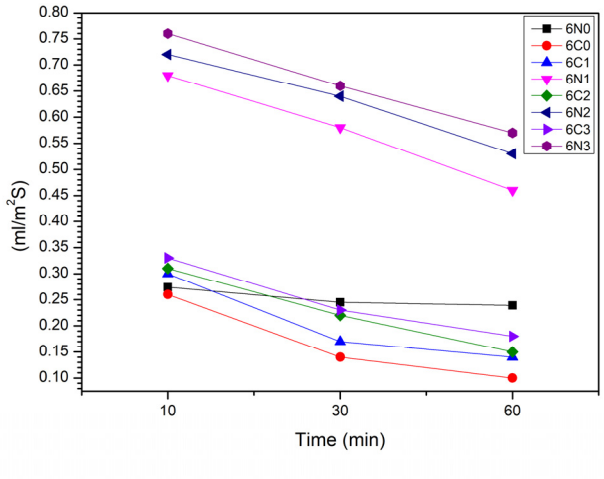

(**a**) C crystalline material

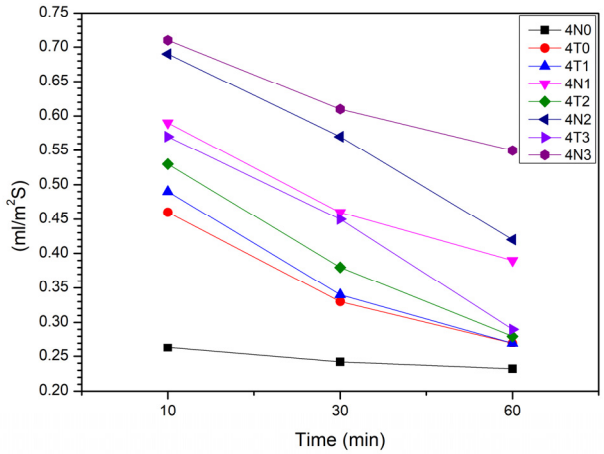

(**b**) T crystalline material

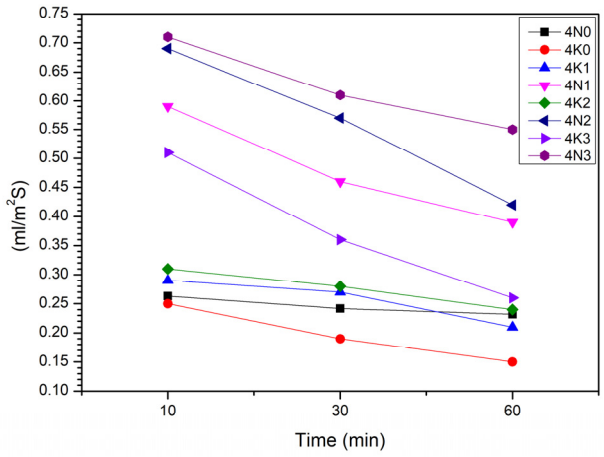

(**c**) K crystalline material

Figure 11. Initial surface water absorption of cement mortar after 56 days when W/C = 0.6.

The aforementioned results indicate that the best surface protection effect can be achieved when using C as the coating material. At the same water–binder ratio and with C as the coating material, the surface water absorption increased with the amount of recycled aggregates. Thus, a superior densification effect cannot be achieved by increasing the amount of substituted recycled materials. The best densification and surface protection effect was achieved when the water–binder ratio was low, C was used as the coating material, and the amount of substitution with recycled materials was 0%. This result corresponded with the results of the saturated water absorption test; thus, the accuracy of the aforementioned result was verified.

As displayed in Figures 6 and 7, when the water–binder ratio was low, we used 20% recycled fine material, and the detection time was 30 min. Under the aforementioned conditions, the surface water absorption of material C after 7 days was 37.5% and 79.17% lower than that of the K and T coatings, respectively. When the water–binder ratio was high, we used 20% recycled fine material, and the detection time was 30 min. Under the aforementioned conditions, the surface water absorption of material C after 7 days was 48.15% and 70.37% lower than that of materials K and T, respectively. Under both the high and low water–binder ratios, recycled fine aggregates could replace 20% of the natural aggregates. The initial surface water absorption was highest for material C, followed by materials K and T. Material C could effectively reduce the surface water absorption of the specimens on which it was coated.

As illustrated in Figures 8 and 9, when the water–binder ratio was low, we used 20% recycled fine material and the detection time was 30 min. Under the aforementioned conditions, the surface water absorption of material C after 28 days was 47.62% and 90.48% lower than that of materials K and T coatings, respectively. When the water–binder ratio was high, we used 20% recycled fine material and the detection time was 30 min. Under the aforementioned conditions, the surface water absorption of material C after 28 days was 54.17% and 79.17% lower than that of materials K and T, respectively. Under both the high and low water–binder ratios, recycled fine aggregates could replace 20% of the natural aggregates. The surface water absorption was highest for material C, followed by materials K and T. Material C effectively reduced the surface water absorption of the specimens on which it was coated.

As shown in Figures 10 and 11, when the water–binder ratio was low, we used 20% recycled fine material, and the detection time was 30 min. Under the aforementioned conditions, the surface water absorption of material C after 56 days was 47.37% and 10.53% lower than that of materials K and T, respectively. When the water–binder ratio was high, we used 20% recycled fine material and the detection time was 30 min. Under the aforementioned conditions, the surface water absorption of material C coating after 56 days was 54.55% and 86.36% lower than that of materials K and T, respectively. Under both the high and low water–binder ratios, recycled aggregates could replace 20% of the natural aggregates. Surface water absorption was highest for material C, followed by materials K and T. Material C effectively reduced the surface water absorption of the samples coated with it.

3.4. Rapid Chloride Penetration Test

According to the standard evaluation of chloride charge flux in the RCPT, cumulative charges of 4000, 2000–4000, 1000–2000, 100–1000, and <100 Coulombs indicate high chloride permeability, medium chloride permeability, low chloride permeability, extremely low chloride permeability, and chloride-free permeation, respectively. The results obtained in the RCPT at the water–binder ratios of 0.4 and 0.6 are displayed in Figures 12 and 13, respectively. The results indicate that the anti-ion permeability was higher at the low water–binder ratio than at the high water–binder ratio. The specimens coated with C had the lowest cumulative total through charge. Material C had high resistance to chloride-ion penetration at both the high and low water–binder ratios. C exhibited the best protective effect among the coating materials, and its chloride-ion penetration resistance was the highest

for 0% replacement of natural aggregates with recycled aggregates. This result is consistent with those of the saturated water absorption and initial surface water absorption tests.

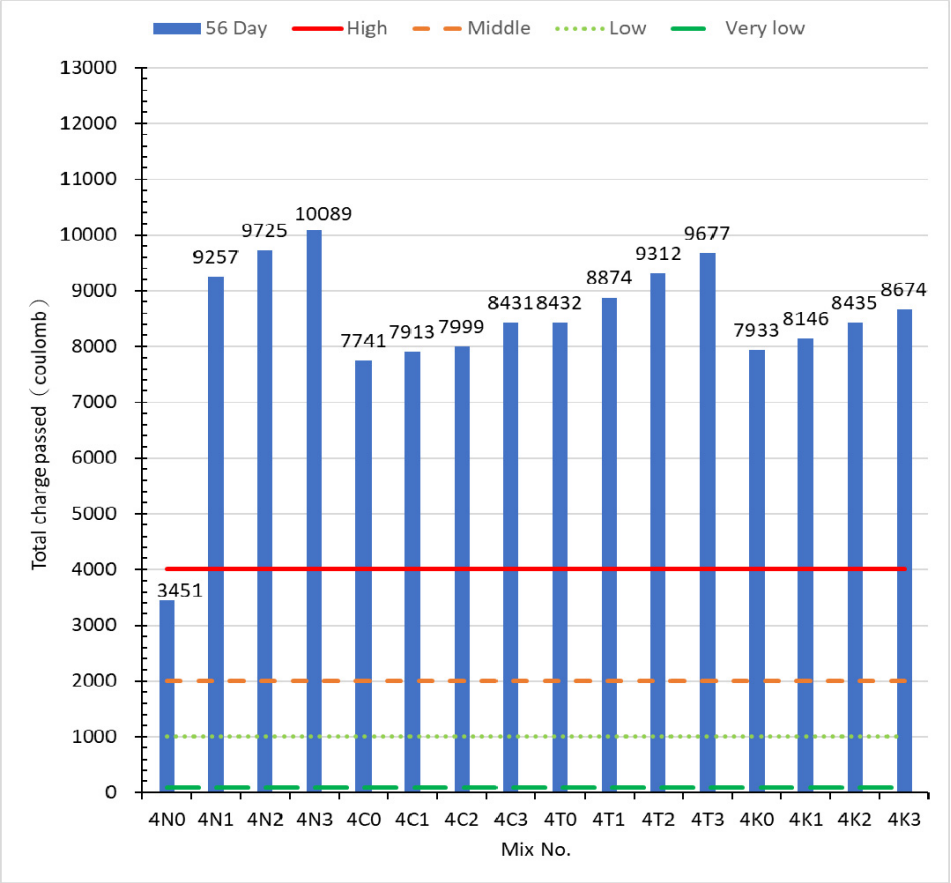

Figure 12. Chloride charge flux of cement mortar when W/C = 0.4.

As displayed in Figure 12, when the water–binder ratio was low, the recycled aggregates could replace 20% of the natural aggregates. The chloride charge flux of material C was 5.45% and 16.41% lower than those of materials K and T, respectively. Moreover, the chloride charge fluxes of the samples coated with materials C, K, and T were 21.58%, 15.29%, and 4.44% lower than those of the uncoated samples, respectively.

As depicted in Figure 13, when the water–binder ratio was high, the recycled aggregates could replace 20% of the natural aggregates. The chloride charge flux of material C was 1.41% and 24.36% lower than those of materials K and T, respectively. The chloride charge fluxes of the samples coated with materials C, K, and T were 58.86%, 56.66%, and 27.75% lower than those of the uncoated samples, respectively.

The resistance to chloride-ion charge flux was highest for material C, followed by materials K and T. Material C effectively resisted chloride-ion penetration.

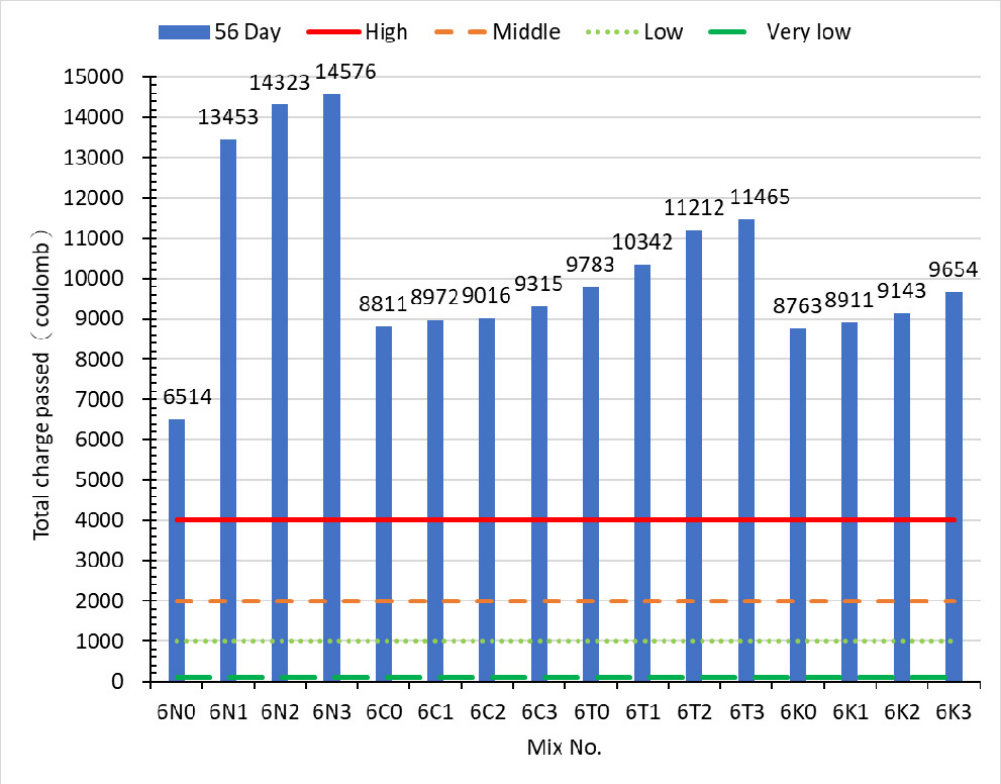

Figure 13. Chloride charge flux of cement mortar when W/C = 0.6.

3.5. MIP Test

The MIP test can be used to determine the distribution of pores in specimens as well as calculate the gel porosity, capillary porosity, and total porosity of specimens. The total pore volume is the pore volume per unit weight of a specimen, and the unit of total pore volume is mL/g. The total pore volume comprises the colloid and capillary pores. Colloid pores, which have a diameter of less than 100 nm, control the stability and durability of the specimen. Capillary pores, which have a diameter of more than 100 nm, control the strength and permeability of a specimen.

The total, colloidal, and capillary pore volumes of the different coating and sealing materials were investigated using water–binder ratios of 0.4 and 0.6 and different proportions of recyclable aggregate replacement. The influence of pozzolan on the cement matrix was also examined. The results of the MIP test are illustrated in Figures 14 and 15. The pore volume of mercury intrusion was smaller at a water–binder ratio of 0.4 than at a water–binder ratio of 0.6. For the specimens containing inorganic crystalline materials, 20% substitution of recyclable aggregates was observed. This result indicated that coating material K had superior pore repairing ability to the other coating materials.

As displayed in Figures 14 and 15, when the water–binder ratio was 0.4, recycled fine aggregates could replace 20% of the natural aggregates. The total pore volume of the material C was 36.08% and 86.87% higher than those of materials K and T, respectively. Compared with the uncoated samples, the total porosities of the samples coated with K, T, and C were 107.38%, 61.45%, and 32.56% lower, respectively. The total pore volume was highest for material K, followed by materials T and C. Material K effectively reduced the total porosity. When the water–binder ratio was 0.6, recycled fine aggregates could replace 20% of the natural aggregates. The total pore volume of material C was 2.59% and 81% lower than those of materials K and T, respectively. Compared with the uncoated samples, the total porosities of the samples coated with T, C, and K were 80.4%, 43.9%, and 40.27% lower, respectively. The total pore volume was largest for material T, followed by materials C and K. Material T effectively reduced the total porosity.

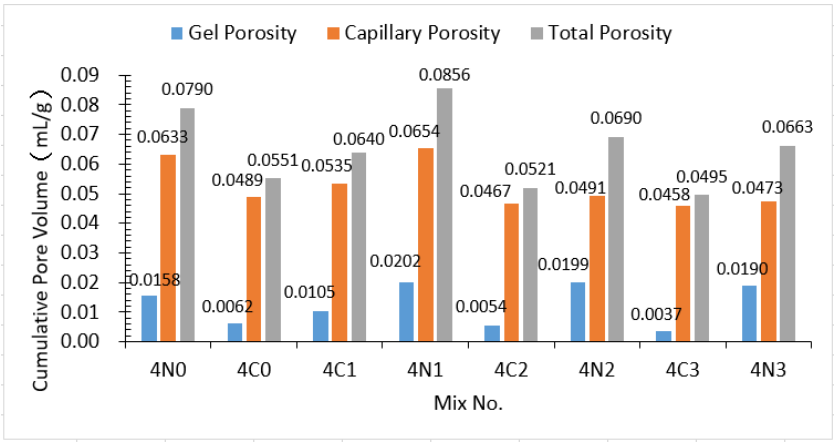

(**a**) C crystalline material

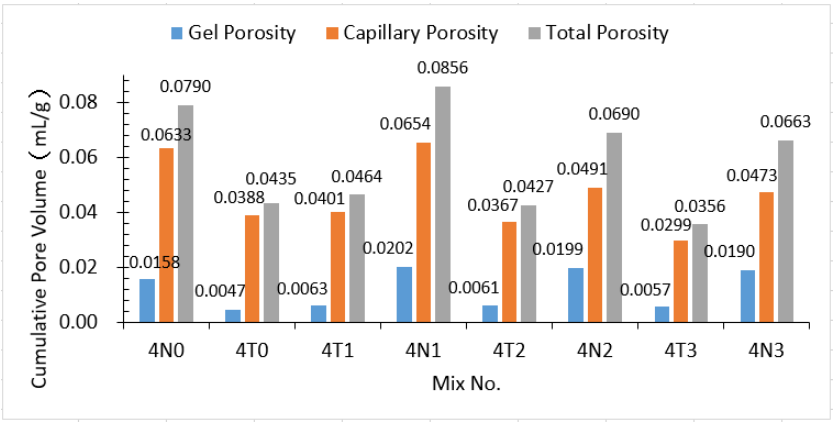

(**b**) T crystalline material

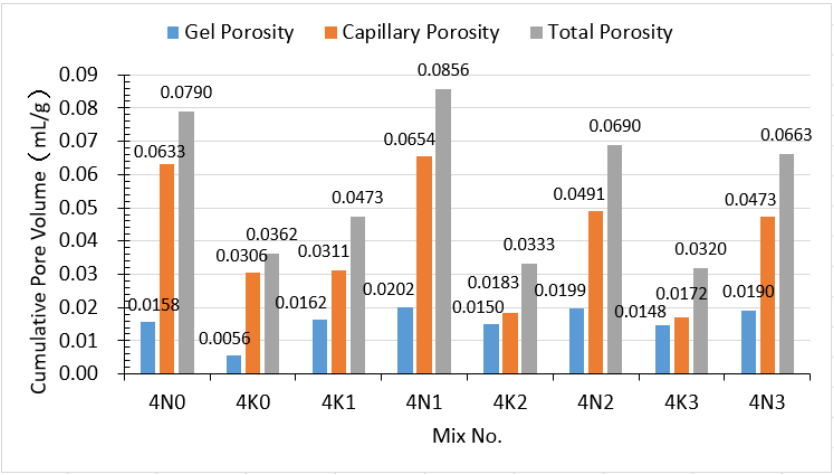

(**c**) K crystalline material

Figure 14. Pore relationships of cement mortar when W/C = 0.4 after 56-day curing.

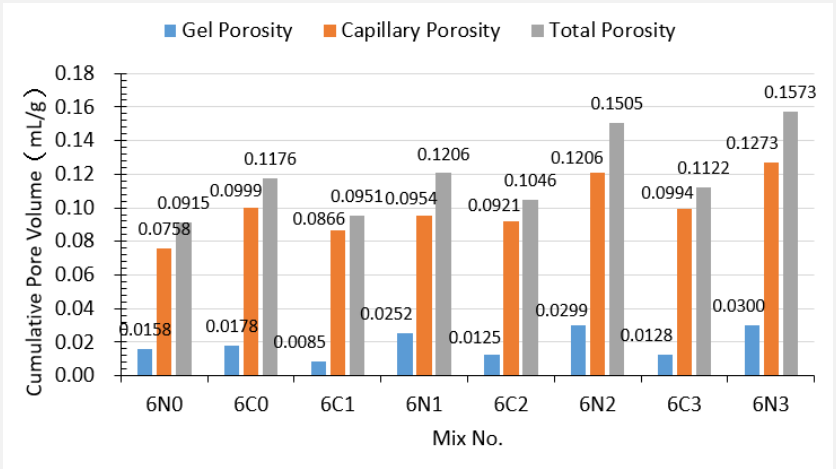

(**a**) C crystalline material

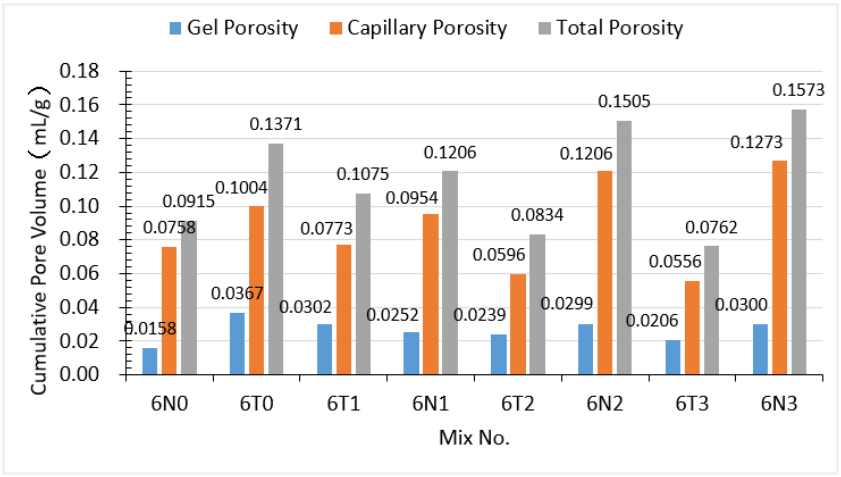

(**b**) T crystalline material

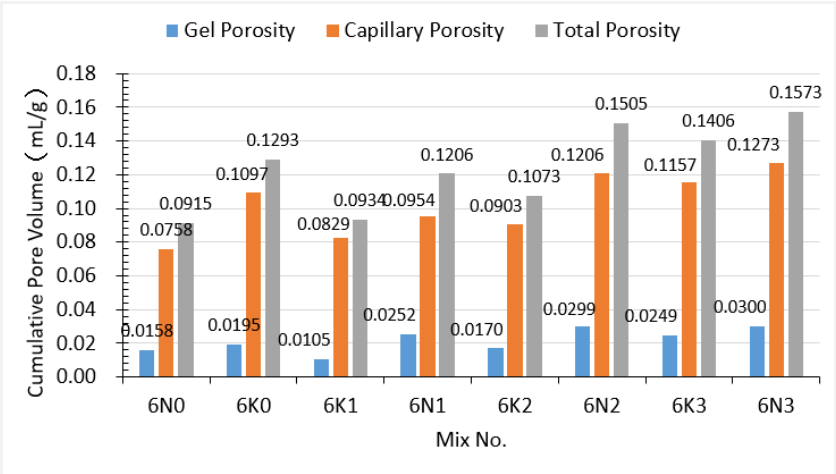

(**c**) K crystalline material

Figure 15. Pore relationships of cement mortar when W/C = 0.6 after 56-day curing.

3.6. Scanning Electron Microscopy

Coatings can form an insoluble crystal structure in the interconnected pores and other voids of concrete. This crystal structure becomes a permanent and integral part of the concrete matrix. Even under a strong hydrostatic pressure, the coating prevents water and other liquids from penetrating into the concrete and protects the concrete from adverse environmental conditions. In this study, dense reticular veins of crystals could be observed in scanning electron microscopy (SEM) images obtained under 3000× magnification.

When material C was used and 20% of the natural aggregates were replaced with recycled aggregates, needle-like structures could be observed 5 mm below the substrate surface under a scanning electron microscope, as displayed in Figures 16 and 17. These needle-like structures were produced by chemical reactions between inorganic coating material and the substrate. X-ray diffraction analysis indicated that the needles consisted of C–S–H colloids or calcium carbonate. As depicted in Figures 18 and 19, no needle-like structures were observed 20 mm below the coating, indicating that the amount of needle-like structures formed decreased with an increase in depth from the coating surface. Material C effectively produced dense network crystals, which effectively resisted chloride-ion penetration as well as reduced water absorption and initial surface water absorption.

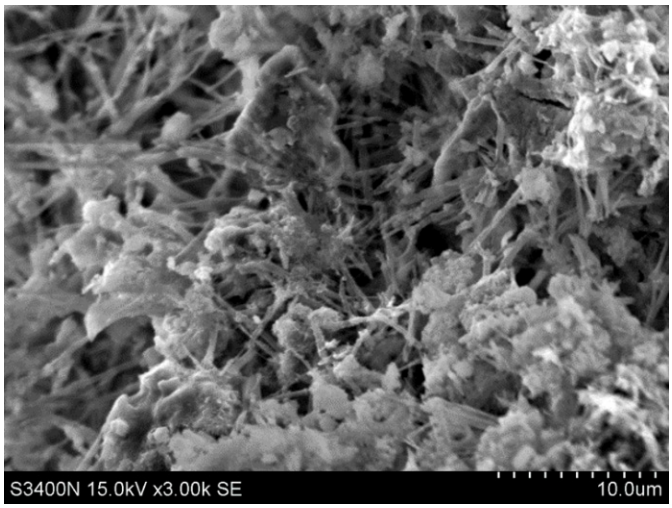

Figure 16. SEM image of microstructures 5 mm below the inner coating of the substrate when W/C = 0.4 (3000×; 4C2, 56 days).

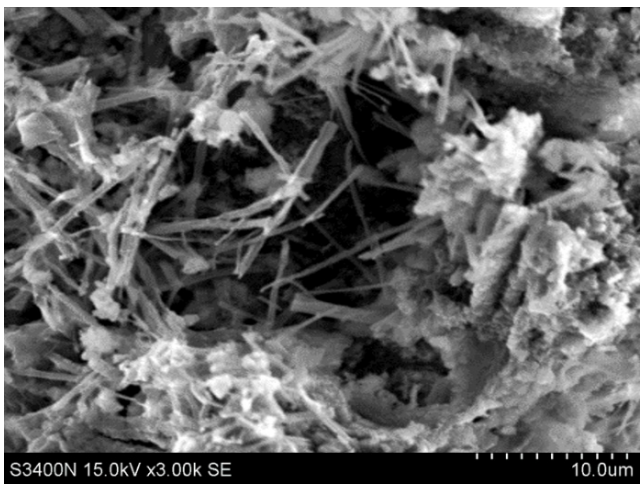

Figure 17. SEM image of the microstructures 5 mm below the inner coating of the substrate when W/C = 0.6 (3000×; 4C2, 56 days).

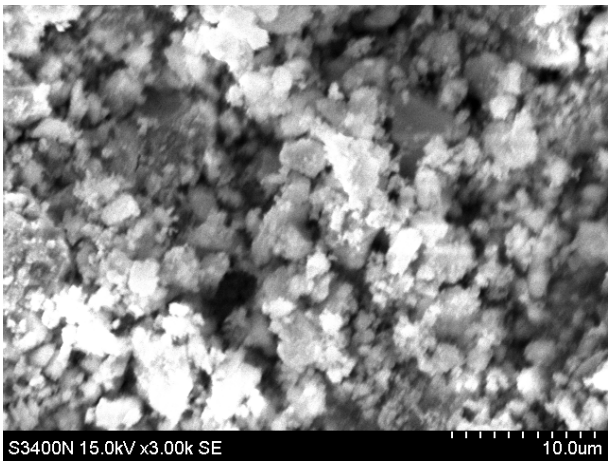

Figure 18. SEM image of the microstructures 20 mm below the inner coating of the substrate when W/C = 0.4 (3000×; 4C2, 56 days).

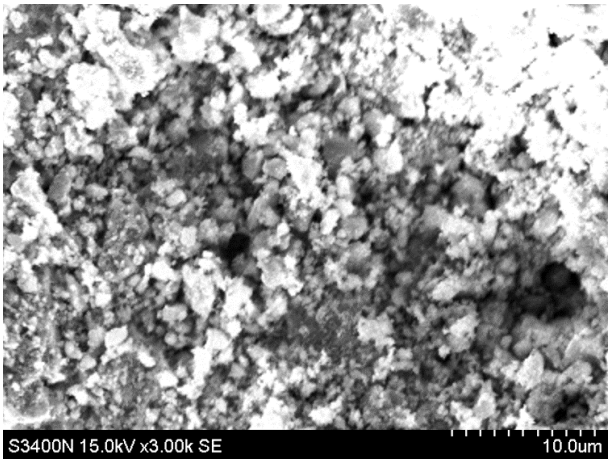

Figure 19. SEM image of the microstructures 20 mm below the inner coating of the substrate when W/C = 0.6 (3000×; 4C2, 56 days).

4. Conclusions

The results of a compressive strength test indicated that specimens coated with material C and containing natural fine aggregates had the highest compressive strength at a low water–binder ratio. This result was confirmed by the results of a permeability test and SEM. The porosity of mortar directly affected the compactness and compressive strength of the specimens. When C was used as the coating material and 20% of the natural aggregates were replaced with recycled fine material, the 28-day compressive strength reached 32.12 MPa, which meets the strength requirement of 30 MPa.

The results of an absorption test indicated that the lower the water absorption, the lower was the internal porosity of the specimens. The best densification effect was achieved at a low water–binder ratio for the specimens coated with C and containing natural fine aggregates. When the water–binder ratio was low, specimens were cured for 28 days, and 20% of the natural aggregates were replaced with recycled aggregates, the water absorption of material C was lower than that of materials K and T.

The results of the initial surface water absorption test and absorption test corresponded to each other. These tests focused on the absorption of cement mortar, and the compactness of the mortar increased with its age. The results of the compressive strength test indicated that the compactness of cement mortar had a positive relationship with its compressive strength.

The results of the RCPT indicated that the lower the porosity, the higher the resistance to chloride ions. Material C effectively resisted chloride-ion penetration. Moreover, the lower the cumulative passing capacity, the higher the resistance to chloride-ion penetration.

The MIP test can be used to examine the changes in the internal porosity of specimens as well as the distribution and amount of capillary and colloidal pores. The results obtained for the mechanical property and permeability tests indicated that the number of pores directly affected the compactness of specimens. The results also indicated that coating material K had good pore repair ability.

SEM analysis indicated that when material C was used, recycled aggregates replaced 20% of the natural aggregates. Needle-like structures were observed 5 mm below the substrate surface at a high and low water–binder ratio. No obvious acicular structure was observed 20 mm below the substrate surface.

Author Contributions: S.-C.C.: Resources, conceptualization, investigation, writing—original sraft, writing—review, and editing. S.-Y.Z.: Resources, methodology, formal analysis, visualization, supervision, validation, writing—review, and editing. H.-M.H.: Data curation, supervision. All authors have read and agreed to the published version of the manuscript.

Funding: This research was funded by East China University of Technology (Project No.: DHBK2019232) and supported by the Ministry of Science and Technology (MOST) in Taiwan under the Grant MOST 109-2221-E-197-006.

Institutional Review Board Statement: Not applicable.

Informed Consent Statement: Not applicable.

Data Availability Statement: Data sharing is not applicable to this article.

Conflicts of Interest: The authors have no conflict of interest to declare.

References

1. Zhang, M.H.; Gjorv, O.E. Effect of silica fume on pore structure and chloride diffusivity of low porosity cement pastes. *Cem. Concr. Res.* **1991**, *21*, 1006–1014. [CrossRef]
2. Mindess, S.; Young, J.F.; Darwin, D. *Concrete*; Prentice Hall: Upper Saddle River, NJ, USA, 2003; pp. 477–504.
3. Sakai, Y. Correlations between air permeability coefficients and pore structure indicators of cementitious materials. *Constr. Build. Mater.* **2019**, *209*, 541–547. [CrossRef]
4. Ballester, P.; Hidalgo, A.; Mármol, I.; Morales, J.; Sánchez, L. Effect of brief heat-curing on microstructure and mechanical properties in fresh cement based mortars. *Cem. Concr. Res.* **2009**, *39*, 573–579. [CrossRef]
5. Wang, X.F.; Zhang, J.H.; Zhao, W.; Han, R.; Han, N.X.; Xing, F. Permeability and pore structure of microcapsule-based self-healing cementitious composite. *Constr. Build. Mater.* **2018**, *165*, 149–162. [CrossRef]
6. Zhang, M. Pore-scale modelling of relative permeability of cementitious materials using X-ray computed microtomography images. *Cem. Concr. Res.* **2017**, *95*, 18–29. [CrossRef]
7. Zhang, M. Relationship between pore structure and chloride diffusion in cementitious materials. *Constr. Build. Mater.* **2019**, *229*, 1–7. [CrossRef]
8. Karimaei, M.; Dabbaghi, F.; Sadeghi-Nik, A.; Dehestani, M. Mechanical performance of green concrete produced with untreated coal waste aggregates. *Constr. Build. Mater.* **2020**, *233*, 1–11. [CrossRef]
9. Wang, Y.; Tan, Y.; Wang, Y.; Liu, C. Mechanical properties and chloride permeability of green concrete mixed with fly ash and coal gangue. *Constr. Build. Mater.* **2020**, *233*, 1–14. [CrossRef]
10. Ouldkhaoua, Y.; Benabed, B.; Abousnina, R.; Kadri, E.-H.; Khatib, J. Effect of using metakaolin as supplementary cementitious material and recycled CRT funnel glass as fine aggregate on the durability of green self-compacting concrete. *Constr. Build. Mater.* **2020**, *235*, 1–11. [CrossRef]
11. Mao, X.; Qu, W.; Zhu, P.; Xiao, J. Influence of recycled powder on chloride penetration resistance of green reactive powder concrete. *Constr. Build. Mater.* **2020**, *251*, 1–8. [CrossRef]
12. Liew, K.M.; Sojobi, A.O.; Zhang, L.W. Green concrete: Prospects and challenges. *Constr. Build. Mater.* **2017**, *156*, 1063–1095. [CrossRef]
13. Huang, R.-Y.; Syu, W.-T.; He, K.-S.; Yu, C.-H. *Benefit/Cost Analysis for Recycling Building Concrete Waste*; Architecture and Building Research Institute, Ministry of Interior: Taipei, Taiwan, 2003.
14. Gholizadeh-Vayghan, A.; Bellinkx, A.; Snellings, R.; Vandoren, B.; Quaghebeur, M. The effects of carbonation conditions on the physical and microstructural properties of recycled concrete coarse aggregates. *Constr. Build. Mater.* **2020**, *257*, 1–11. [CrossRef]

15. Chen, Q. Research on the Effect of Polycrystalline Silicon Powder on the Properties of Recycled Cement Matrix Materials. Master's Thesis, Institute of Civil Engineering, National Ilan University, Ilan, Taiwan, 2017.
16. Sim, J.; Park, C. Compressive strength and resistance to chloride ion penetration and carbonation of recycled aggregate concrete with varying amount of fly ash and fine recycled aggregate. *Waste Manag.* **2011**, *31*, 2352–2360. [CrossRef] [PubMed]
17. Zega, C.J.; Di Maio, Á.A. Use of recycled fine aggregate in concretes with durable requirements. *Waste Manag.* **2011**, *31*, 2336–2340. [CrossRef]
18. Geng, J.; Sun, J. Characteristics of the carbonation resistance of recycled fine aggregate concrete. *Constr. Build. Mater.* **2013**, *49*, 814–820. [CrossRef]
19. Song, M.; Jiaping, L.; Wei, L.; Yaocheng, W.; Jianzhong, L.; Liang, S.; Qian, J. Property and microstructure of aluminosilicate inorganic coating for concrete: Role of water to solid ratio. *Constr. Build. Mater.* **2017**, *148*, 846–856.
20. *Cementitious Capillary Crystalline Waterproof Material*; National Standards of the People's Republic of China: Beijing, China, 2012; GB 18445-2012.
21. Kameche, Z.A.; Ghomari, F.; Choinska, M.; Khelidj, A. Assessment of liquid water and gas permeabilities of partially saturated ordinary concrete. *Constr. Build. Mater.* **2014**, *65*, 551–565. [CrossRef]
22. Shi, L.; Liu, J.Z.; Liu, J.P. Effect of polymer coating on the properties of surface layer concrete. *Procedia Eng.* **2012**, *27*, 291–300. [CrossRef]
23. Freitag, S.A.; Bruce, S.M. *The Influence of Surface Treatments on the Service Lives of Concrete Bridges*; NZ Transport Agency Research Report 403: Wellington, New Zealand, 2010.
24. Du, H. Using Mercury Porosimeter to Explore the Pore Structure of Cementitious Materials. Master's Thesis, Institute of Civil Engineering and Disaster Prevention, China Institute of Technology, Sanhe, China, 2009.
25. Power, T.C. The Physical Structure of Portland Cement Paste. *Chem. Cem.* **1964**, *1*, 391–416.
26. Almusallam, A.A.; Khan, F.M.; Dulaijan, S.U.; Al-Amoudi, O.S.B. Effectiveness of surface coatings in improving concrete durability. *Cem. Concr. Compos.* **2003**, *25*, 473–481. [CrossRef]
27. Li, J. Research on Pore Structure and Corrosion Behavior of Cementitious Composites with Silica Fume and Fly Ash. Ph.D. Dissertation, Institute of Materials Engineering, National Taiwan Ocean University, Keelung, Taiwan, 2013.
28. Zhang, P.; Folker, H.W.; Vogel, M.; Harald, S.M.; Zhao, T. Influence of freeze-thaw cycles on capillary absorption and chloride penetration into concrete. *Cem. Concr. Res.* **2017**, *100*, 60–67. [CrossRef]
29. Cosoli, G.; Mobili, A.; Giulietti, N.; Chiariotti, P.; Pandarese, G.; Tittarelli, F.; Bellezze, T.; Mikanovic, N.; Revel, G.M. Performance of concretes manufactured with newly developed low-clinker cements exposed to water and chlorides: Characterization by means of electrical impedance measurements. *Constr. Build. Mater.* **2021**, *271*, 1–12. [CrossRef]
30. Ho, H.-L.; Huang, R.; Lin, W.-T.; Cheng, A. Pore-structures and durability of concrete containing pre-coated fine recycled mixed aggregates using pozzolan and polyvinyl alcohol materials. *Constr. Build. Mater.* **2018**, *160*, 278–292. [CrossRef]
31. Jalilifar, H.; Sajedi, F. Micro-structural analysis of recycled concretes made with recycled coarse concrete aggregates. *Constr. Build. Mater.* **2021**, *267*, 1–10. [CrossRef]
32. Danish, A.; Mosaberpanah, M.A. Influence of cenospheres and fly ash on the mechanical and durability properties of high-performance cement mortar under different curing regimes. *Constr. Build. Mater.* **2021**, *279*, 1–20. [CrossRef]
33. Chen, S.-C.; Huang, R.; Hsu, H.-M.; Zou, S.-Y.; Teng, L.W. Evaluation of Penetration Depth and Protective Effec-Tiveness of Concrete-Penetrating Sealer Materials. *J. Mar. Sci. Technol.* **2016**, *24*, 244–249. [CrossRef]
34. Zou, S. Evaluation of Protective Effectiveness and Crystalline Mechanism of Concrete Surface Penetrating Sealer. Ph.D. Dissertation, Department of Harbor and River Engineering, National Taiwan Ocean University, Keelung, Taiwan, 2012.
35. *Standard Specification for Concrete Aggregates*; ASTM International: West Conshohocken, PA, USA, 2018; ASTM C33/C33M-18.
36. *Standard Test Method for Relative Density (Specific Gravity) and Absorption of Fine Aggregate*; ASTM International: West Conshohocken, PA, USA, 2015; ASTM C128-15.
37. *Standard Test Method for Compressive Strength of Cylindrical Concrete Specimens*; American Society for Testing and Materials: West Conshohocken, PA, USA, 2013; ASTM C39/C39M–12a.
38. *Standard Test Method for Density, Absorption, and Voids in Hardened Concrete*; ASTM International: West Conshohocken, PA, USA, 2013; ASTM C642-13.
39. *Testing Concrete—Part 208: Recommendations for the Determination of the Initial Surface Absorption of Concrete*; The British Standards Institution: London, UK, 1996; BS 1881-208.
40. *Standard Test Method for Electrical Indication of Concrete's Ability to Resist Chloride Ion Penetration*; American Society for Testing and Materials: West Conshohocken, PA, USA, 2012; ASTM C1202-12.
41. *Standard Test Method for Determination of Pore Volume and Pore Volume Distribution of Soil and Rock by Mercury Intrusion Porosimetry*; American Society for Testing and Materials: West Conshohocken, PA, USA, 2010; ASTM D4404–10.
42. Diamanti, M.V.; Brenna, A.; Bolzoni, F.; Berra, M.; Pastore, T.; Ormellese, M. Effect of polymer modified cementitious coatings on water and chloride permeability in concrete. *Constr. Build. Mater.* **2013**, *49*, 720–728. [CrossRef]